


RESEARCH ARTICLE

Regulation of myofilament force and loaded shortening by skeletal myosin binding protein C

 Joel C. Robinett¹, Laurin M. Hanft¹, Janelle Geist², Aikaterini Kontrogianni-Konstantopoulos² , and Kerry S. McDonald¹ 

Myosin binding protein C (MyBP-C) is a 125–140-kD protein located in the C-zone of each half-thick filament. It is thought to be an important regulator of contraction, but its precise role is unclear. Here we investigate mechanisms by which skeletal MyBP-C regulates myofilament function using rat permeabilized skeletal muscle fibers. We mount either slow-twitch or fast-twitch skeletal muscle fibers between a force transducer and motor, use Ca²⁺ to activate a range of forces, and measure contractile properties including transient force overshoot, rate of force development, and loaded sarcomere shortening. The transient force overshoot is greater in slow-twitch than fast-twitch fibers at all Ca²⁺ activation levels. In slow-twitch fibers, protein kinase A (PKA) treatment (a) augments phosphorylation of slow skeletal MyBP-C (sMyBP-C), (b) doubles the magnitude of the relative transient force overshoot at low Ca²⁺ activation levels, and (c) increases force development rates at all Ca²⁺ activation levels. We also investigate the role that phosphorylated and dephosphorylated sMyBP-C plays in loaded sarcomere shortening. We test the hypothesis that MyBP-C acts as a brake to filament sliding within the myofilament lattice by measuring sarcomere shortening as thin filaments traverse into the C-zone during lightly loaded slow-twitch fiber contractions. Before PKA treatment, shortening velocity decelerates as sarcomeres traverse from ~3.10 to ~3.00 μm. After PKA treatment, sarcomeres shorten a greater distance and exhibit less deceleration during similar force clamps. After sMyBP-C dephosphorylation, sarcomere length traces display a brief recoil (i.e., “bump”) that initiates at ~3.06 μm during loaded shortening. Interestingly, the timing of the bump shifts with changes in load but manifests at the same sarcomere length. Our results suggest that sMyBP-C and its phosphorylation state regulate sarcomere contraction by a combination of cross-bridge recruitment, modification of cross-bridge cycling kinetics, and alteration of drag forces that originate in the C-zone.

Introduction

The canonical regulatory pathway of striated muscle contraction involves Ca²⁺ activation of the thin filaments (McKillop and Geeves, 1993). More recent studies have provided evidence for a thick filament-mediated model (Linari et al., 2015) that regulates contraction in concert with thin filament regulation. According to the new model, the thick filament transitions between an OFF and ON state as a function of stress. In the absence of Ca²⁺ and when load is minimal, both thin and thick filaments reside in the OFF state. Upon initial Ca²⁺ activation of the thin filament, the thick filament remains in the OFF state; however, there is a small population of cross-bridges (~5%) that are modeled to be constitutively primed for activation. These constitutively activated myosin motors are capable of driving lightly loaded shortening (Piazzesi et al., 2007). However, once an external load is applied to the muscle, the actively cycling cross-bridges generate stress throughout the thick filament,

which triggers the transition of the thick filament to the ON state and unlocks a much larger population of cross-bridges to contract against high loads. It has been proposed that MyBP-C may regulate the level of thick filament activation (Kampourakis et al., 2014), and thus MyBP-C may be critical in determining the dynamic efficiency of striated muscle.

MyBP-C is a ~125- to ~140-kD elongated, flexible polypeptide (~40 nm × ~3 nm) with low α-helical and high proline content (Hartzell and Sale, 1985). MyBP-C has been localized in striated muscle to seven to nine transverse stripes spaced ~43 nm apart throughout the inner two-thirds of each half thick filament, i.e., a region known as the C-zone (Pepe and Drucker, 1975; Craig and Offer, 1976; Bennett et al., 1986). There are several MyBP-C isoforms encoded by different genes and expressed in both a development- and muscle-specific manner (Craig and Offer, 1976; Yamamoto and Moos, 1983; Wang et al., 2018). MyBP-C

¹Department of Medical Pharmacology and Physiology, School of Medicine, University of Missouri, Columbia, MO; ²Department of Biochemistry and Molecular Biology, School of Medicine, University of Maryland, Baltimore, MD.

Correspondence to Kerry S. McDonald: mcdonaldks@missouri.edu

This work is part of a special collection on myofilament function.

© 2019 Robinett et al. This article is distributed under the terms of an Attribution–Noncommercial–Share Alike–No Mirror Sites license for the first six months after the publication date (see <http://www.rupress.org/terms/>). After six months it is available under a Creative Commons License (Attribution–Noncommercial–Share Alike 4.0 International license, as described at <https://creativecommons.org/licenses/by-nc-sa/4.0/>).

contains several immunoglobulin-like and fibronectin-like domains numbered C0 to C10 (Flashman et al., 2004; Barefield and Sadayappan, 2010; Harris et al., 2011). The skeletal isoforms of MyBP-C lack the C0 domain (Ackermann and Kontrogianni-Konstantopoulos, 2013). Each MyBP-C isoform has a proline-alanine rich domain at its N terminus and a conserved MyBP-C-specific motif (i.e., the M-domain) between C1 and C2. Phosphorylation of the slow-skeletal MyBP-C (sMyBP-C) primarily occurs within the Pro/Ala-rich region (i.e., serine [Ser]-59, Ser-62, and threonine [Thr]-84), and to a lesser degree in the M-domain (Ser-204), while it is currently unknown if the fast skeletal isoform of MyBP-C (fMyBP-C) is modulated via phosphorylation (Ackermann and Kontrogianni-Konstantopoulos, 2011; Wang et al., 2018). Both Ser-59 and Ser-62 of sMyBP-C are modulated by PKA, while Thr-84 is modulated by PKC, and Ser-204 is modulated by both kinases (Ackermann and Kontrogianni-Konstantopoulos, 2011). In all isoforms of MyBP-C, the C-terminal domains exhibit a longitudinal orientation, suggesting that domains C10 to C8 lie parallel to the thick filament surface while the N terminus (C7-C0) can run perpendicular to the thick filament and extend toward thin filaments (Moos et al., 1978; Yamamoto, 1986; Luther et al., 2011; Reconditi et al., 2014; Lee et al., 2015). Interestingly, in vitro studies show that the N-terminal region of MyBP-C including the M-domain binds myosin at both the S2-S1 junction and the S1 neck region (Starr and Offer, 1978; Ababou et al., 2008; Bhuiyan et al., 2012) and, in addition, both cardiac and skeletal MyBP-C isoforms are capable of binding actin with micromolar affinity (Moos et al., 1978; Yamamoto, 1986; Shaffer et al., 2009; Kensler et al., 2011), which may give rise to an internal drag that impedes loaded shortening (Previs et al., 2012; Walcott et al., 2015). The capability of MyBP-C to bind both thin and thick filaments makes it well suited as a regulatory molecule, especially considering the findings that these interactions can be modulated by phosphorylation of its N-terminal region (Rybakova et al., 2011; van Dijk et al., 2014; Moss et al., 2015; Kensler et al., 2017).

The goal of this study was to pursue a deeper understanding of sMyBP-C's role in regulation of muscle contraction. We tested the hypothesis that sMyBP-C acts as an attenuator of contractile force and shortening, which can be, in part, alleviated by PKA-induced phosphorylation. According to this idea, dephosphorylation of sMyBP-C would tend to depress activation due to a structural constraint of cross-bridges and slow loaded shortening by its interaction with actin, while phosphorylation of sMyBP-C would enhance activation due to release of a structural constraint of myosin cross-bridges and speed loaded shortening by alleviating the drag imposed by its binding to the thin filament. This was addressed by making mechanical measurements in single permeabilized slow-twitch skeletal muscle fibers, which provided a platform for addressing sMyBP-C's regulatory role in a structurally intact myofibrillar lattice replete with the array of sarcomeric proteins.

Materials and methods

Experimental animals

All procedures involving animals were performed in accordance with the Animal Care and Use Committee of the University of

Missouri. Male Sprague-Dawley rats (~2–4 mo old), obtained from Envigo RMS, were housed in groups of two and provided food and water ad libitum.

Solutions

Relaxing solution for permeabilized skeletal muscle fibers contained 1 mM DTT, 100 mM KCl, 10 mM imidazole, 2.0 mM EGTA, 4.0 mM ATP, and 1 mM (free, 5 total) MgCl₂. Minimal Ca²⁺ activating solution (pCa 9.0) for experimental protocol contained 7.00 mM EGTA, 20 mM imidazole, 5.42 mM MgCl₂, 72.37 mM KCl, 0.016 mM CaCl₂, 14.50 mM PCr, and 4.7 mM ATP. Maximal Ca²⁺ activating solution (pCa 4.5) for experimental protocol contained 7.00 mM EGTA, 20 mM imidazole, 5.26 mM MgCl₂, 60.25 mM KCl, 7.01 mM CaCl₂, 14.50 mM PCr, and 4.81 mM ATP. A range of Ca²⁺ concentrations for experiments was prepared by varying combinations of maximal and minimal Ca²⁺ solutions. Preactivating solution contained 0.5 mM EGTA, 20 mM imidazole, 5.42 mM MgCl₂, 98.18 mM KCl, 0.016 mM CaCl₂, 14.50 mM PCr, and 4.8 mM ATP. PKA solution was prepared by diluting 1 mg DTT in 100 μl of ultrapure water; the DTT solution was then added to 400 U PKA (Sigma), and the 100 μl PKA was then diluted in 700 μl pCa 9.0 solution to yield 0.5 U PKA/μl. Lambda phosphatase solution (New England Biolabs) was prepared by a 100-fold dilution into pCa 9.0 solution to yield 4 U lambda phosphatase/μl.

Skeletal muscle fiber preparations

Slow-twitch and fast-twitch skeletal muscle fibers were obtained from Sprague-Dawley rats anesthetized by inhalation of isoflurane (0.5 ml isoflurane: 4.5 ml olive oil) and subsequently euthanized by excision of the heart. Slow-twitch skeletal muscle fibers were obtained from the soleus muscle, whereas the fast-twitch skeletal muscle fibers were obtained from the psoas muscle. The muscles were isolated and placed in relaxing solution. Bundles of muscle fibers were separated and tied to capillary tubes. They were stored in the freezer in a 1:1 ratio of relaxing solution and glycerol for up to 1 mo. On the day of experimentation, single fibers were dissected from a bundle by gently pulling fibers from the end of the bundle (McDonald, 2000). A summary of fiber characteristics is provided in Table 1.

Experimental apparatus

Prior to mechanical measurements, the experimental apparatus was mounted on the stage of an inverted microscope (model IX-70; Olympus Instrument Co.), which was placed on a pneumatic vibration isolation table. Mechanical measurements were performed using a capacitance gauge force transducer (Model 403, sensitivity of 20 mV/mg and resonant frequency of 600 Hz; Aurora Scientific). Length changes were presented to one end of the fiber via a DC torque motor (model 308c; Aurora Scientific) driven by voltage commands from a personal computer via a 16-bit D/A converter (AT-MIO-16E-1; National Instruments Corp.). Fibers were attached between the force transducer and length motor by placing the ends of the fiber into stainless steel troughs (25 gauge). The fiber ends were secured by overlaying a ~0.5-mm length of 3-0 monofilament suture (Ethicon). The suture secured the fiber into the troughs by tightening two loops of

Table 1. **Skeletal muscle fiber preparation characteristics**

Fibers	Length (μm)	Width (μm)	SL (μm)	Passive tension (kN/m^2)	Maximal Ca^{2+} -activated tension (kN/m^2)
Slow-twitch fibers ($n = 18$)	$1,071 \pm 38$	76 ± 2	2.43 ± 0.02	0.66 ± 0.09	121 ± 6
Fast-twitch fibers ($n = 9$)	$1,104 \pm 85$	92 ± 3	2.43 ± 0.04	0.25 ± 0.03	145 ± 4

10-0 monofilament (Ethicon) at each end (Fig. 1 A). The attachment procedure was performed under a stereomicroscope (90 \times zoom). Force and length signals were digitized at 1 kHz and stored on a personal computer using Lab-View for Windows (National Instruments Corp.). Simultaneous sarcomere length measurements of force and length were obtained via IonOptix SarcLen system, which used a fast-Fourier transform algorithm of the video image of the fiber (Fig. 1 B). The region of interest is $\sim 220 \times 30 \mu\text{m}$; therefore, the sarcomere length is calculated from approximately one tenth of the permeabilized skeletal muscle fiber preparation.

Slack–restretch protocol

All mechanical measurements of skeletal muscle fibers were performed at $14 \pm 1^\circ\text{C}$. Following attachment, the relaxed skeletal muscle fiber preparation was adjusted to a sarcomere length (SL) of $\sim 2.40 \pm 0.1 \mu\text{m}$ by manual manipulation of the length micrometer on fiber mount. The preparation was first transferred into pCa 4.5 solution for maximal Ca^{2+} activation then subsequently transferred into a series of submaximal Ca^{2+} activating solutions, ending back in pCa 4.5 maximal activating solution. At each pCa, steady-state tension was allowed to develop and the fiber was rapidly slacked ($\sim 15\%$ original muscle length) and allowed to shorten for ~ 20 ms, after which the preparation was restretched to a value slightly greater than the original muscle length for ~ 2 ms and then returned to original muscle length (Fig. 1 C). The sarcomere length tracking was lost when the fiber was slacked, causing an arbitrary reading by the IonOptix system (Figs. 2 A and 4 A). The fibers underwent approximately three slack–restretch maneuvers at each Ca^{2+} activation level. Forces in submaximal activating solutions were expressed as a fraction of force obtained during maximal Ca^{2+} activation. The maximal force value was calculated as an average of maximal force at the beginning and end of the experiment. To assess the effects of PKA-induced phosphorylation of sMyBP-C on the transient force overshoot, rate of force redevelopment, and transient force decay rate, the aforementioned slack–restretch protocol was performed before and after a 60-min incubation with PKA or lambda phosphatase solution. Ca^{2+} -activating solutions were adjusted to elicit desired relative forces ($\sim 25\%$, 50% , 75% , and maximal activation); the same submaximal activating pCa solutions were used following PKA treatment in the respective fibers.

Loaded shortening/lengthening protocol

Permeabilized slow-twitch skeletal muscle fibers were placed in activating solution and adjusted to an SL in which the thin filaments were outside of the C-zone (SL $\sim 3.15 \mu\text{m}$). The fibers were Ca^{2+} activated to ~ 30 – 40% maximal force. Then a series of force clamps (less than steady-state force) were performed to drive the

thin filaments into the C-zone (starting at SL ~ 3.08 – $3.04 \mu\text{m}$; Reconditi et al., 2014). Using a servo-system, force was maintained constant for a designated period of time (~ 700 ms; Fig. 1 F) while sarcomere length was continuously monitored via the IonOptix SarcLen system (Fig. 1, B and H). Following the force clamp, the fiber preparation was slacked to reduce force to near zero to allow estimation of the relative load sustained during isotonic shortening; the fiber was then reextended to its initial length (Fig. 1 F). Repeated measures were performed before and after PKA and/or lambda phosphatase treatment.

Western blots

The level of residue-specific phosphorylation of sMyBP-C was assessed using SDS-PAGE followed by Western blotting. A glycerinated fiber bundle containing ~ 20 fibers was isolated and cut into three equally sized sections, which were each placed into separate tubes containing $20 \mu\text{l}$ of relaxing solution and incubated with $5 \mu\text{l}$ of either 20 U PKA (Sigma), $2,000$ U lambda phosphatase (New England Biolabs), or relaxing solution and incubated for 1 h at room temperature ($\sim 20^\circ\text{C}$). The reaction was stopped by the addition of $25 \mu\text{l}$ of SDS-sample buffer. The samples then underwent SDS-PAGE using 12% polyacrylamide slab gels. After SDS-PAGE, the gels were placed on prewetted nitrocellulose membranes sandwiched between several sheets of 3MM chromatography paper, and protein samples were transferred to nitrocellulose using a semidry blot apparatus at constant current (120 mA) for 1.5 h. Immediately following transfer, the blots were stained with Ponceau S (Pierce) to verify equivalent protein loads and then placed in blocking buffer consisting of 5% dry milk, pH 7.4, and rocked for 1 h. The blots were then placed in small bags containing primary phospho-specific antibodies against Ser-59 and Ser-204 of sMyBP-C (Ackermann and Kontrogianni-Konstantopoulos, 2011) diluted 1:500 in blocking buffer and incubated overnight at room temperature ($\sim 20^\circ\text{C}$). Blots were then washed in blocking buffer and incubated for 2 h with secondary peroxidase-conjugated goat anti-rabbit antibodies (Thermo Fisher Scientific) diluted 1:1,000 in blocking buffer. Blots were then washed with PBS and subsequently coated with Supersignal West Pico-chemiluminescent substrate (Pierce) and imaged using a Bio-Rad ChemDoc imaging system, and signal intensity was quantified using ImageJ software (National Institutes of Health).

Data analysis

Force redevelopment traces were fitted with a double exponential equation:

$$F = F_r + A(1 - e^{-k_1x}) + B(1 - e^{-k_2x}),$$

where F is force during force redevelopment, F_r is the residual force before redevelopment, A is the force contributing to the

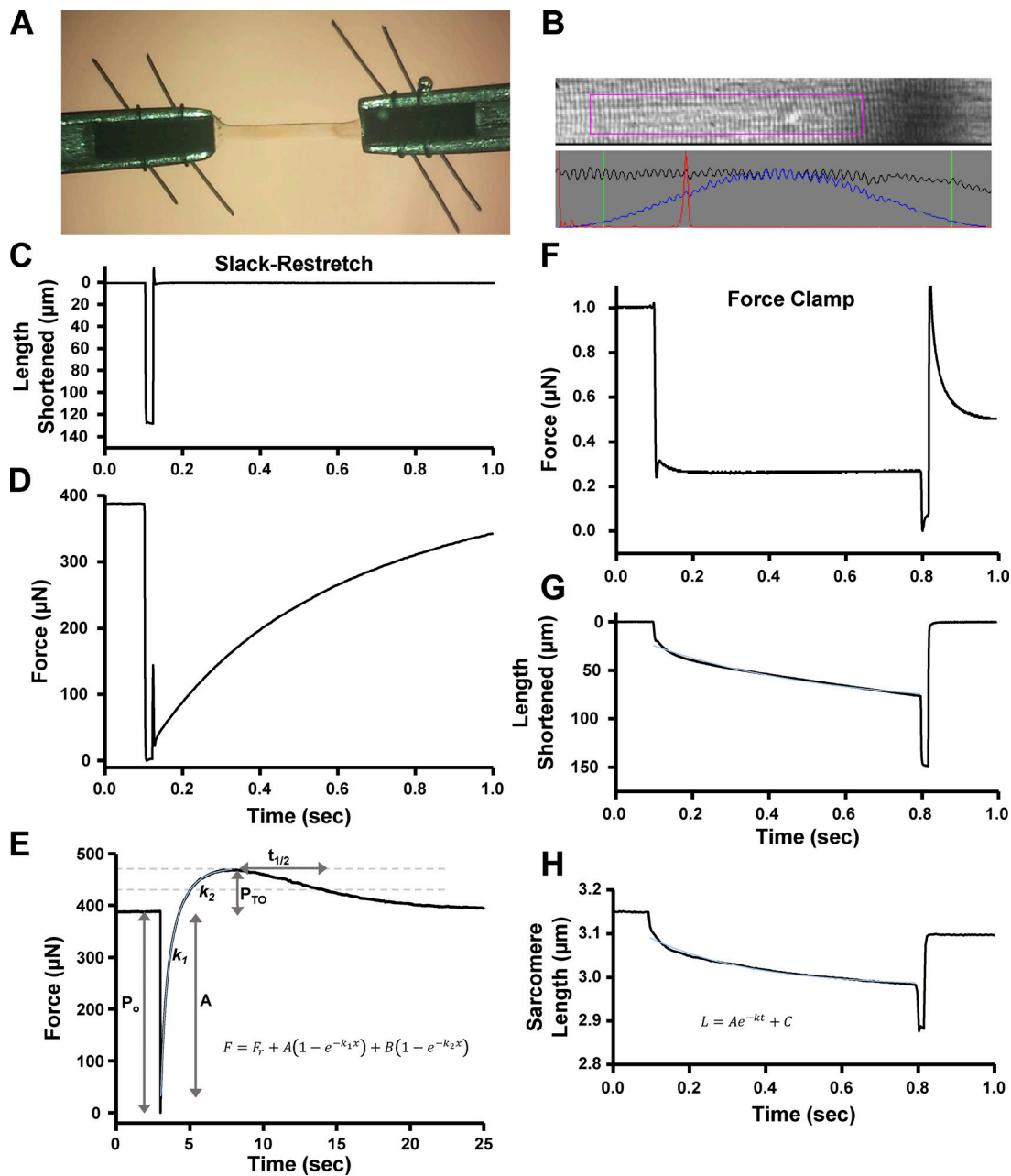


Figure 1. **Analysis of permeabilized skeletal muscle fiber mechanics.** (A) A permeabilized slow-twitch or fast-twitch skeletal muscle fiber (~1,000 μm long) was mounted between a motor and a force transducer. (B) Sarcomere length was monitored via IonOptix SarcLen system, which used a fast-Fourier transform algorithm of the video image of the fiber. (C and D) Muscle fiber length (C) and force (D) during a slack–restretch protocol. The muscle fiber was allowed to develop steady-state tension at each pCa, then the fiber was rapidly slacked (~15% original muscle length) and restretched to original muscle length to elicit force redevelopment from near-zero tension. (E) Schematic of force redevelopment analysis (see Materials and methods for further description). (F–H) Force (F), muscle length (G), and sarcomere length (H) are shown during a submaximal force clamp. Permeabilized slow-twitch skeletal muscle fibers were adjusted to a sarcomere length in which the thin filaments were outside of the C-zone (SL ~3.15 μm) and Ca^{2+} activated to ~30–40% maximal force. Then a series of submaximal force clamps were performed to drive thin filaments into the C-zone (see Fig. 7 A). (H) Schematic of analysis of sarcomere length trace during loaded shortening (see Materials and methods for description of analysis). Fitted curves (in light blue) are shown in E, G, and H.

first exponential phase, k_1 is the rate constant of force redevelopment of this first exponential phase, and B is the force contributing to the second exponential phase with a rate constant of k_2 . Force redevelopment was fitted from F_r to the force maximum. Force redevelopment traces provided various force characteristic values (Fig. 1 E). Permeabilized

skeletal muscle fiber preparations first were submerged in Ca^{2+} -activating solutions and allowed to rise to steady-state isometric force (P_o). Following the slack–restretch maneuver, force often redeveloped transiently to a different maximal force ($P_o + P_{TO}$). Values for transient force overshoots were calculated by subtracting isometric force from the maximal

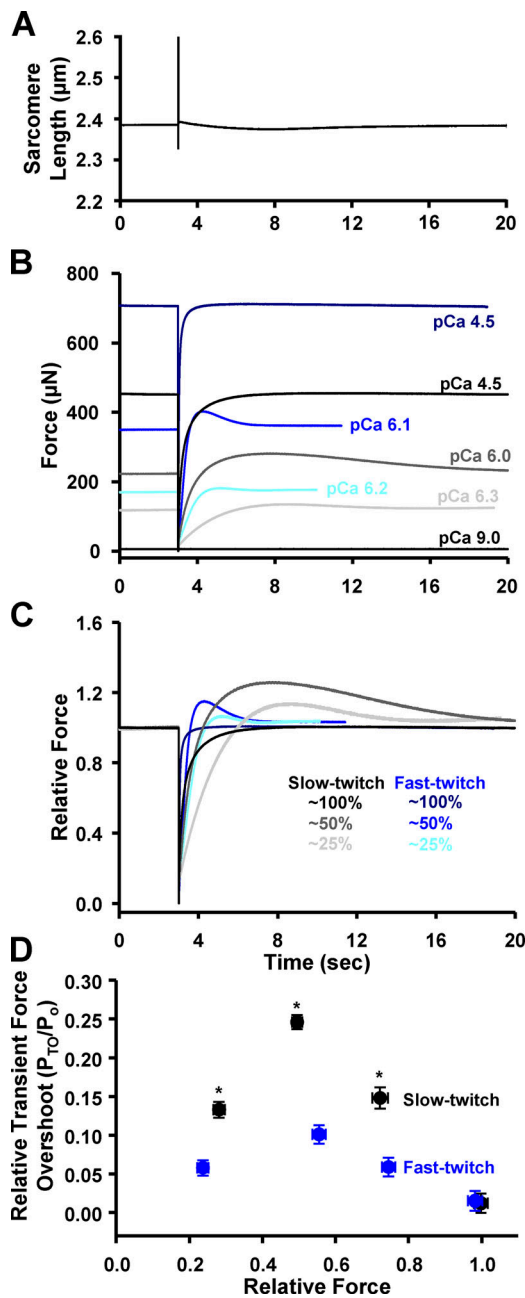


Figure 2. Transient force overshoots in slow-twitch and fast-twitch skeletal muscle fibers. (A) Representative sarcomere length trace during a slack-restretch maneuver. (Of note, the sarcomere length pattern is unresolved during the slackened period.) (B) Representative absolute force traces following a slack-restretch maneuver from a slow-twitch (black, charcoal, gray) and a fast-twitch (navy, blue, aqua) skeletal muscle fiber. (C) Force traces normalized to steady-state force before the mechanical perturbation. (D) P_{TO} was expressed as a fraction of steady-state force (P_o) before the slack-restretch maneuver. By two-way ANOVA, within slow-twitch ($n = 5$) and fast-twitch ($n = 4$) fiber groups, all P_{TO}/P_o points were significantly different from each other except at ~25% versus ~75% forces. *, $P < 0.05$, slow-twitch fibers versus fast-twitch fibers.

redeveloped force ($P_{TO} = (P_o + P_{TO}) - P_o$) (Fig. 1 E). Transient force overshoots were analyzed relative to isometric force and expressed as P_{TO}/P_o . Rates of transient force decay were calculated as follows:

$t_{1/2}$ = time from maximal force to when force =

$$\frac{0.95 * [(P_o + P_{TO}) - P_o]}{2}$$

Loaded shortening traces were fitted to a single decaying exponential equation (from the onset to the end of the force clamp):

$$L = Ae^{-kt} + C,$$

where L is the sarcomere length during loaded shortening, t is time, A is a constant of length, k is a curvature constant of the sarcomere length trace, and C is the initial sarcomere length (Fig. 1, G and H).

Statistical analysis

Two-way ANOVA was used to compare interactions between Ca^{2+} activation levels and fiber types on relative transient force overshoot (P_{TO}/P_o), rate constants of force redevelopment, and $t_{1/2}$ values. A Student-Newman-Keuls test was used for all pairwise comparisons among different groups. Paired t tests were used to compare the effects of PKA and lambda phosphatase on contractile properties. Values are expressed as means \pm SEM. $P < 0.05$ is accepted as significant.

Results

Ca^{2+} dependence of transient force overshoot in rat permeabilized skeletal muscle fibers

Previous work found evidence that transient force overshoot resulted from, at least in part, an increase in cooperative activation processes, including recruitment of force-generating cross-bridges (Campbell, 2006b). If, indeed, cooperative recruitment of cross-bridges is a mechanism for transient force overshoot, it stands to reason that fast-twitch skeletal muscle fibers would have a greater magnitude of transient force overshoot compared with relatively less cooperative slow-twitch skeletal muscle fibers (McDonald, 2000). We directly tested this hypothesis by quantifying Ca^{2+} dependence of transient force overshoot in rat slow-twitch and fast-twitch skeletal muscle fibers. Skeletal muscle fiber preparations were activated to elicit 25%, 50%, 75%, and 100% (maximal) Ca^{2+} activation, and once steady-state force was reached, a slack-restretch maneuver was performed. Force redevelopment after the slack-restretch maneuver was often associated with a transient force overshoot (P_{TO} ; Fig. 2). Both slow-twitch and fast-twitch skeletal muscle fibers exhibited a Ca^{2+} activation dependence of relative transient force overshoot (P_{TO}/P_o ; Fig. 2 D). Half-maximal (i.e., 50%) Ca^{2+} activation elicited the greatest magnitude of P_{TO}/P_o , while maximal activation elicited a negligible P_{TO}/P_o in both fiber types (Fig. 2 D). Contrary to our hypothesis, force redevelopment in slow-twitch fibers elicited greater relative transient force overshoot than the more cooperative fast-twitch fibers over the spectrum of Ca^{2+} activation levels (Fig. 2). This suggests that slow-twitch skeletal muscle has a greater capacity for cooperative cross-bridge recruitment in response to mechanical perturbations than fast-twitch skeletal muscle. There was not a fiber-type dependence of P_{TO} at maximal Ca^{2+} activation, which is thought to arise from a lack of additional cross-bridges

available for force generation following slack–restretch maneuver.

Force redevelopment rates in slow versus fast-twitch fibers

Force development rates were characterized throughout the entire transient force overshoot process. Traditionally, force redevelopment traces have been fitted with a single exponential equation over a 1-s time frame (Campbell, 2006b; Stelzer and Moss, 2006; Hanft and McDonald, 2009). We found that force redevelopment over several seconds, which includes the rising portion of the transient force overshoot, was better fitted by a double exponential equation. The double exponential fit implies that two distinct molecular processes are involved in force development of skeletal muscle myofilaments. As summarized in Fig. 3, force redevelopment traces often included an early fast phase (quantified with the rate constant, k_1) followed by a slower phase, enumerated with the rate constant, k_2 (Fig. 1 E). Fast-twitch muscle fibers elicited faster rates of force redevelopment than slow-twitch muscle fibers over the entire range of Ca^{2+} activation. Interestingly, in both fiber types, the two different processes of force redevelopment converged into one process at low Ca^{2+} activation levels (Fig. 3, A and B). The rate constant of the fast process (k_1) was highly Ca^{2+} activation dependent, while the slower process (k_2) was independent of Ca^{2+} activation levels. The convergence of force redevelopment processes suggests that at low Ca^{2+} activations only one of the two molecular processes is dominant in force generation.

Force decay rates

The rate of force decay was assessed in both slow-twitch and fast-twitch skeletal muscle fibers. In this study, force decay rates were quantified as the time to half decay of transient force overshoot ($t_{1/2}$). Similar to force redevelopment rates, fast-twitch skeletal muscle fibers had faster decay rates than slow-twitch fibers as evident by significantly lower $t_{1/2}$ values (Fig. 3 C). However, slow-twitch muscle fibers exhibited greater Ca^{2+} activation dependence of force decay rate than fast-twitch fibers. In slow-twitch fibers, $t_{1/2}$ values at ~25% and ~50% relative force were significantly different from all other values; in fast-twitch fibers, only the $t_{1/2}$ value at maximal Ca^{2+} activations was greater than other values. The lower Ca^{2+} dependence of transient force decay rates in fast-twitch fibers may be due to a myofibrillar system that has evolved to inactivate both the thin and thick filaments in a highly coordinated, cooperative switch-like fashion, which would assist in rapid relaxation, allowing for explosive contractions needed to optimize fast-twitch muscle performance.

sMyBP-C phosphorylation state effects on force transients after slack–restretch

Next we addressed the potential regulatory role that PKA-mediated phosphorylation of myofilament proteins, in particular sMyBP-C, plays in the contractile properties of slow-twitch skeletal muscle fibers. Our laboratory has previously observed that PKA-induced phosphorylation of cMyBP-C and cardiac troponin I (cTnI) elicited marked increases in transient force overshoot in permeabilized cardiac myocyte preparations

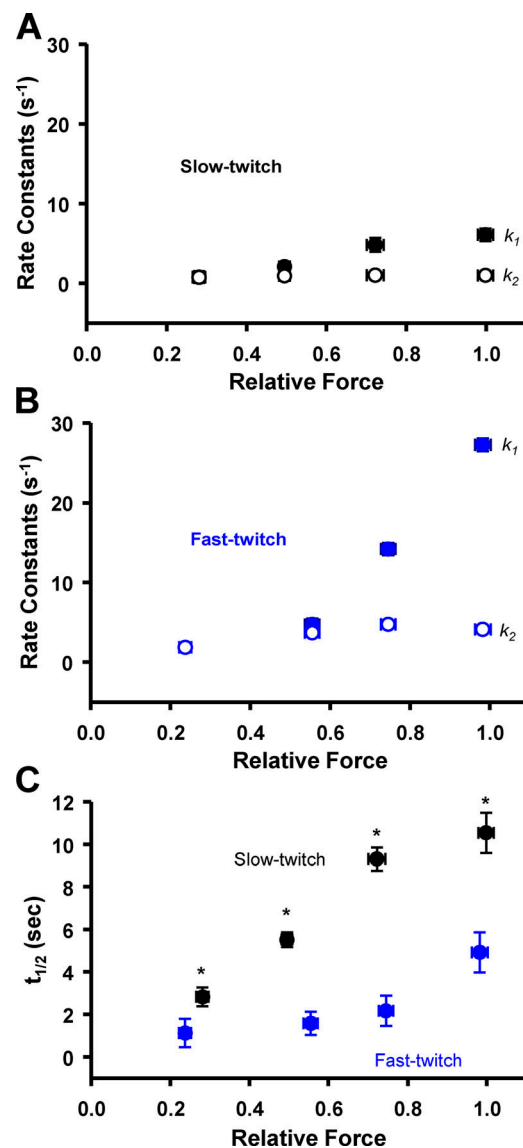


Figure 3. Force redevelopment and decay rates. (A and B) Rate constants (s^{-1}) from a double exponential (k_1 and k_2) fit across relative forces in slow-twitch (A; black; $n = 5$) and fast-twitch (B; blue; $n = 4$) fibers. Values for k_1 were highly dependent on Ca^{2+} activation levels, while k_2 values were similar over the entire range of Ca^{2+} activation levels in both fiber types. Values for k_1 at ~75% and ~100% relative force were significantly different from all other values in both fiber types. (C) $t_{1/2}$ was Ca^{2+} activation dependent in a manner qualitatively similar to the k_1 rate constant. In slow-twitch fibers, the $t_{1/2}$ at ~25% and ~50% relative force was significantly different from all other values. In fast-twitch fibers, the $t_{1/2}$ at ~100% relative force was significantly greater than all other values. *, $P < 0.05$ slow-twitch fibers versus fast-twitch fibers.

(Hanft and McDonald, 2009). To address the molecule specificity of this phenomenon, we treated slow-twitch skeletal muscle fibers with PKA, which we previously showed to phosphorylate sMyBP-C but not slow-skeletal cTnI (Hanft et al., 2016). In the current study, PKA was observed to phosphorylate sMyBP-C at both Ser-59 and Ser-204 by Western blot analysis (Fig. 4 E), as previously reported (Ackermann and Kontogianni-Konstantopoulos, 2011). We hypothesized that

PKA treatment would increase P_{TO} , since there is evidence that phosphorylation of MyBP-C, at least in cardiac muscle, relieves constraint on myosin heads (Colson et al., 2008, 2012; Kensler et al., 2017). We tested the effects of PKA treatment on force redevelopment traces and quantified the transient force overshoot over a range of Ca^{2+} activation levels. Relative transient force overshoot magnitude (P_{TO}/P_o) was unchanged following PKA treatment at 50%, 75%, and maximal Ca^{2+} activation levels, i.e., P_{TO}/P_o values were similar before and after PKA treatment at these Ca^{2+} activation levels (Fig. 4). However, at low Ca^{2+} activation levels, the relative transient force overshoot significantly increased after PKA treatment (Fig. 4). P_{TO}/P_o values increased from ~19% before PKA to ~45% after PKA treatment at low Ca^{2+} activation levels (Fig. 4 D). PKA had no effect on the magnitude of transient force overshoot in fast-twitch skeletal muscle fibers (not depicted). Alternatively, following lambda phosphatase treatment, which was shown to lower sMyBP-C phosphorylation (Fig. 4 E), transient force overshoot was decreased at low (25%) and medium (50%) Ca^{2+} activation levels (Fig. 6 A).

In slow-twitch fibers, PKA treatment yielded a significant increase in the rates of force redevelopment at all Ca^{2+} activation levels (Fig. 5). In fact, PKA increased the rates for both the fast phase (k_1) and the slower phase (k_2) of force redevelopment (Fig. 5, A and B). These findings suggest that the phosphorylation of sMyBP-C per se speeds the processes that control myofilament force generation, which has been supported in previous cardiac muscle and slow skeletal muscle fiber studies (Patel et al., 2001; Gresham et al., 2014; Hanft et al., 2016; Mamidi et al., 2016). In a manner similar to force redevelopment rates, transient force decay rates tended to be faster after PKA treatment. However, $t_{1/2}$ was significantly lower only at 50% activation after PKA (Fig. 5 C). Of note, $t_{1/2}$ values were much more variable at the 75% Ca^{2+} activation compared with lower Ca^{2+} activation levels, and there were no $t_{1/2}$ values at maximal Ca^{2+} activation, since transient force overshoot was absent during maximal activation. Lambda phosphatase caused a decrease in the rates of both the fast phase (k_1 , Fig. 6 B) and the slower phase (k_2 , Fig. 6 C) of force redevelopment over the entire range of Ca^{2+} activation. For fast-twitch fibers, we did not observe PKA treatment to have any effect on either the rates of force development or force decay times (not depicted); thus, subsequent experiments investigating the effects of sMyBP-C phosphorylation state on sarcomere shortening/lengthening used only slow-twitch skeletal muscle fibers.

PKA effects on filament sliding into the C-zone

To study the hypothesis that sMyBP-C imposes an internal drag on sliding filaments within the context of the myofilament lattice, we designed experiments whereby permeabilized slow-twitch skeletal muscle fibers were stretched to SLs at which the thin filaments were just outside of the C-zone (SL ~3.08–3.04 μm ; Fig. 7 A; Craig and Offer, 1976; Greaser and Pleitner, 2014; Reconditi et al., 2014). The C-zone was estimated to extend ~500 nm from the middle of the M line (Pepe and Drucker, 1975; Bennett et al., 1986; Lee et al., 2015). Thin filament lengths were estimated to be ~1.02–1.05 μm from a study in rat skeletal muscle (Greaser and Pleitner, 2014). Then,

during submaximal Ca^{2+} activation, the fiber underwent lightly loaded (~10–30% isometric force) shortening whereby the thin filaments were driven into the C-zone (i.e., sarcomere shortening from ~3.15 to ~3.00 μm). As the sarcomeres shortened over this range, the SL recordings displayed a curvilinear pattern, implying a deceleration as thin filaments entered the C-zone (Fig. 7 B). This was quantified as an increase in the curvature (k) of the sarcomere shortening trace (Fig. 7 C). After PKA treatment, there was a decrease in the curvature (k) of the sarcomere traces (Fig. 7 C), which suggests a decrease in the internal drag imposed on the filaments by sMyBP-C. Further evidence of sMyBP-C's role in regulating filament sliding was obtained by quantifying the distance of sarcomere shortening during load clamps. Sarcomere shortening distance (i.e., ΔSL) increased following PKA treatment (Fig. 7 D). Together, these results are consistent with sMyBP-C binding to actin and imposing an internal drag that opposes shortening, and this drag is alleviated by PKA-mediated phosphorylation of sMyBP-C.

Lambda phosphatase affects the internal drag imposed on filament sliding

Next, the effects of dephosphorylation of sMyBP-C on sarcomere shortening were addressed by treating fibers with lambda phosphatase. Lambda phosphatase reduced sMyBP-C phosphorylation according to Western blot analysis using primary phospho-specific antibodies against sMyBP-C Ser-59 and Ser-204 (Fig. 4 E). Previous work has reported that lambda phosphatase treatment caused a marked slowdown in thin filament sliding upon entry into the C-zone of isolated thick filaments (Previs et al., 2012). We undertook a similar experimental approach but in the context of an intact sarcomeric myofilament lattice. Following lambda phosphatase, there was a decrease in ΔSL during load clamps (Fig. 7 D). In addition, after treating slow-twitch skeletal muscle fibers with lambda phosphatase, we often observed a “bump” in the sarcomere length trace during lightly loaded contractions. The bump occurred at sarcomere lengths that, in theory, should be where sliding thin filaments should first engage the C-zone (i.e., SL = ~3.08 to ~3.04 μm ; Fig. 8 B). We also observed that the timing of the bump in the sarcomere length trace could be adjusted by altering the relative force under which the fiber shortened. When the force clamp was slightly decreased, the bump occurred sooner, whereas a slight increase in the force clamp caused a greater delay before the bump (Fig. 8 C). Importantly, the onset of the bump was observed at the same sarcomere length irrespective of the force clamp and the time to reach the aforementioned sarcomere length. This result is consistent with sMyBP-C creating an internal load that the thin filaments encounter as they enter the C-zone. Such a load appears to briefly cause the thin filaments to cease sliding toward the middle of the sarcomere and elicits a slight recoil of the thin filaments toward the ends of the sarcomere. A final series of experiments was performed to further test the idea that sMyBP-C can impart a drag on myofilament sliding. For these experiments, supra-isometric force clamps were imposed that caused the fiber to lengthen. We observed biphasic lengthening when fibers were stretched under load from a sarcomere length of ~3.03 to ~3.07 μm ; i.e., the

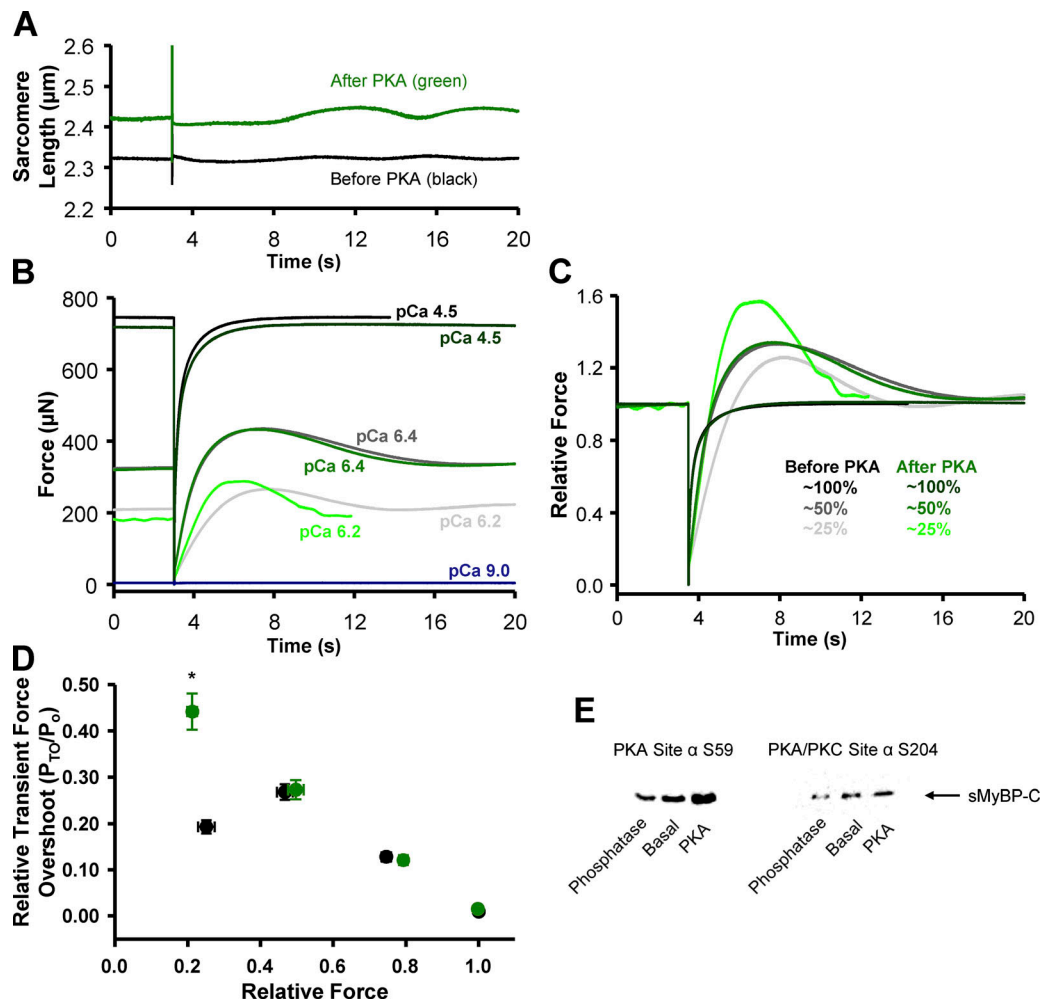


Figure 4. Transient force overshoot in slow-twitch skeletal muscle fibers before and after PKA treatment. (A) Representative sarcomere length trace during a slack–restretch maneuver in a permeabilized slow-twitch skeletal muscle fiber before (black) and after (green) PKA treatment. (B) Representative absolute force traces following a slack–restretch maneuver from a permeabilized slow-twitch skeletal muscle fiber before (black, charcoal, gray) and after (forest, green, lime) PKA at 25% (pCa 6.4), 50% (pCa 6.2), and maximal (pCa 4.5) relative force, respectively. (C) Representative relative force traces, which were normalized to the steady-state force before the mechanical perturbation. (D) Relative transient force overshoot (P_{TO}/P_o) in permeabilized slow-twitch skeletal muscle fiber preparations before (black) and after (green) PKA treatment as a function of Ca^{2+} activation levels ($n = 4$). P_{TO}/P_o was significantly increased only at low Ca^{2+} activation levels. *, $P < 0.05$ using paired t test analysis. (E) Amino acid residue-specific phosphorylation levels of sMyBP-C in a slow-twitch skeletal muscle fiber bundle under basal conditions and after either lambda phosphatase or PKA treatment. Following lambda phosphatase sMyBP-C Ser59 and Ser204 phosphorylation (relative to basal) was 0.70 ± 0.05 and 0.72 ± 0.05 , respectively ($n = 6$). Following PKA, sMyBP-C Ser59 and Ser204 phosphorylation (relative to basal) was 1.58 ± 0.17 and 1.27 ± 0.03 , respectively ($n = 6-8$).

lengthening accelerated over this sarcomere length range (Fig. 8 D). On the other hand, if the sarcomere length started at $\sim 3.08 \mu m$ (i.e., thin filaments were outside the C-zone) then supra-isometric force clamps elicited more linear sarcomere length traces. These results are consistent with the outer boundary of the C-zone being localized at a sarcomere length of $\sim 3.05 \mu m$ in this fiber preparation and sMyBP-C eliciting a drag force, which is alleviated when thin filaments exit the C-zone.

Discussion

This study examined dynamic contractile properties in rat permeabilized slow-twitch and fast-twitch skeletal muscle fibers, in an attempt to further elucidate subcellular mechanisms that regulate striated muscle contraction. The main findings

from these experiments were (a) relative transient force overshoot was greater in less cooperative slow-twitch skeletal muscle fibers compared with fast-twitch skeletal muscle fibers, suggesting that transient force overshoot is not determined by inherent myofilament cooperativity of activation alone (Fig. 2 D); (b) in slow-twitch fibers, PKA treatment caused a doubling of the relative transient force overshoot, but only at low Ca^{2+} activation levels, suggesting a mechanism whereby phosphorylation of sMyBP-C relieves its constraint on myosin heads under low stress conditions (Fig. 4 D); (c) PKA treatment of slow-twitch skeletal muscle fibers increased the rates of force development at all Ca^{2+} activation levels, suggesting that phosphorylation of sMyBP-C accelerates myosin cross-bridge cycling kinetics (Fig. 5, A and B); and (d) dephosphorylation of sMyBP-C resulted in a deceleration of shortening and a brief recoil in

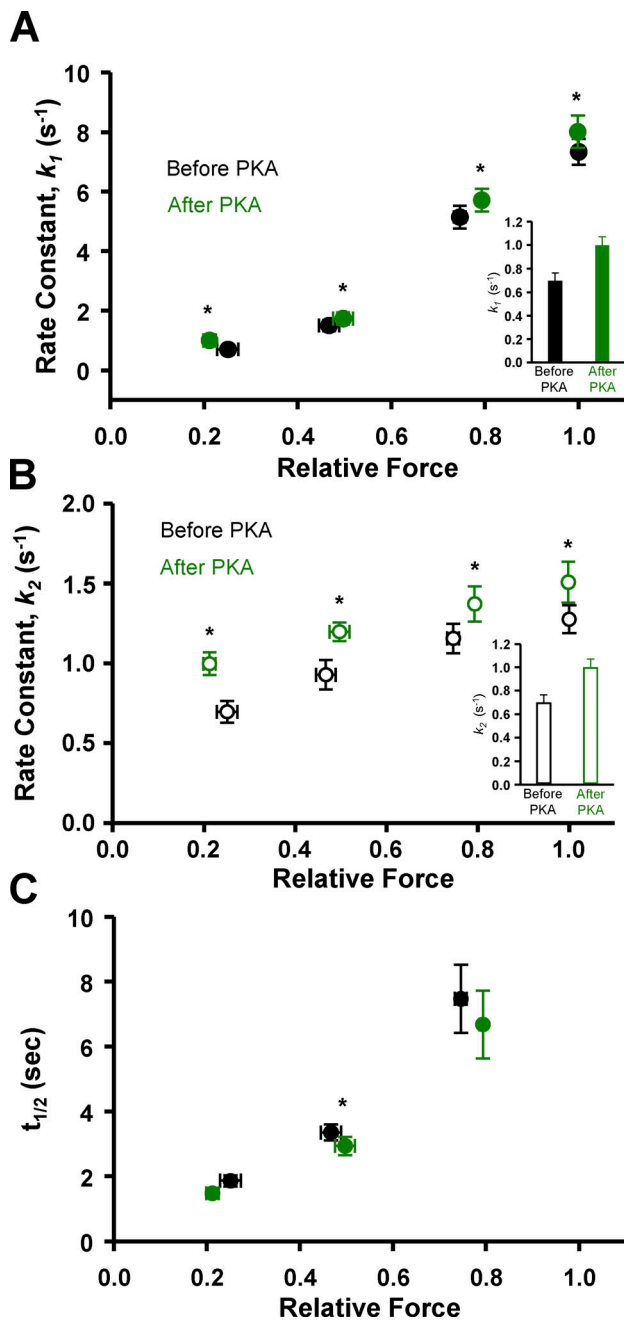


Figure 5. Force redevelopment and decay rates in permeabilized slow-twitch skeletal muscle fiber preparations before (black) and after (green) PKA treatment as a function of Ca²⁺ activation levels. (A and B) PKA increased the rate constants (s⁻¹) of both the fast phase (k_1 , A) and slow phase (k_2 , B) of force redevelopment at all Ca²⁺ activation levels. Values at low relative force levels are shown in insets. (C) $t_{1/2}$ following PKA treatment had the tendency of being faster; however, it was only significantly faster at 50% Ca²⁺ activation. There was no $t_{1/2}$ at maximum Ca²⁺ activation due to the lack of a transient force overshoot ($n = 4$). *, $P < 0.05$ using paired t test analysis.

sarcomeres at SLs that approximate where the thin filaments enter the C-zone (SL = ~3.08–3.04 μm ; Fig. 8). This latter finding suggests the presence of a substantive internal load that can oppose myofilament sliding, which is alleviated by the phosphorylation of sMyBP-C. Collectively, these results suggest that

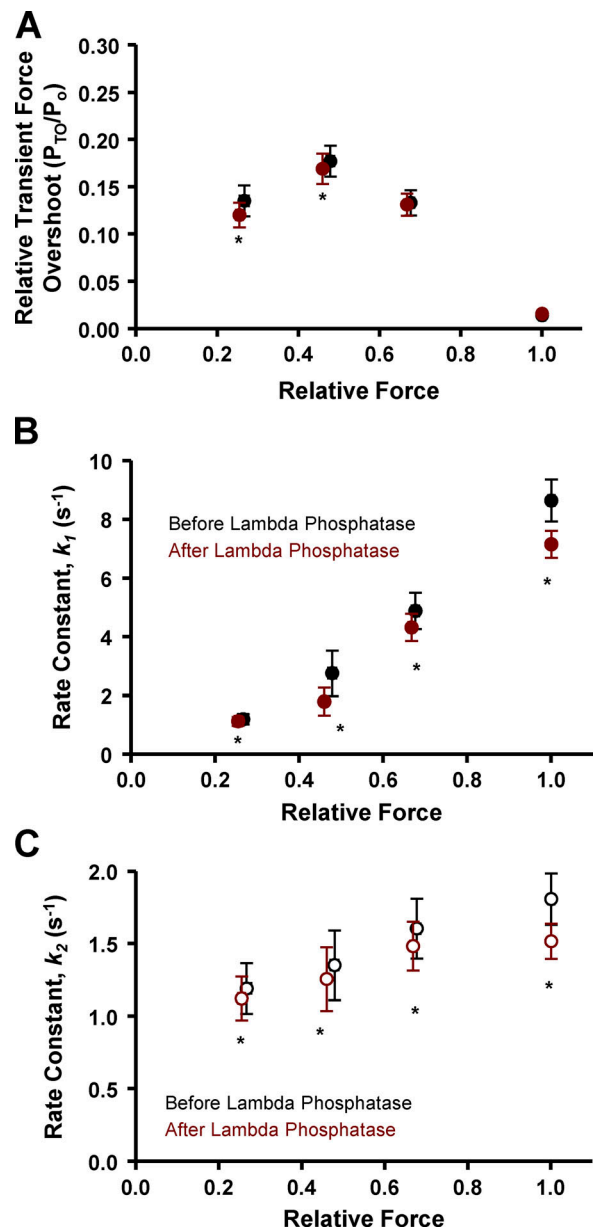


Figure 6. Transient force overshoot and force redevelopment rates in permeabilized slow-twitch skeletal muscle fiber preparations before (black) and after (red) lambda phosphatase treatment as a function of Ca²⁺ activation levels. (A) Relative transient force overshoot (P_{TO}/P_o) was significantly decreased at low and medium (25% and 50%) Ca²⁺ activation levels following lambda phosphatase (red). (B and C) Lambda phosphatase decreased the rate constants (s⁻¹) of both the fast phase (k_1 , B) and slow phase (k_2 , C) of force redevelopment at all Ca²⁺ activation levels ($n = 4$). *, $P < 0.05$ using paired t test analysis.

sMyBP-C and its phosphorylation state regulate sarcomere contraction by a combination of recruiting cross-bridges, modifying cross-bridge cycling kinetics, and altering internal drag forces in the C-zone and tend to oppose myofilament force, loaded shortening, and power output.

For this study, we chose to focus on skeletal muscle fibers and their functional regulation by sMyBP-C for the following reasons: (a) acute functional properties such as fatigue and

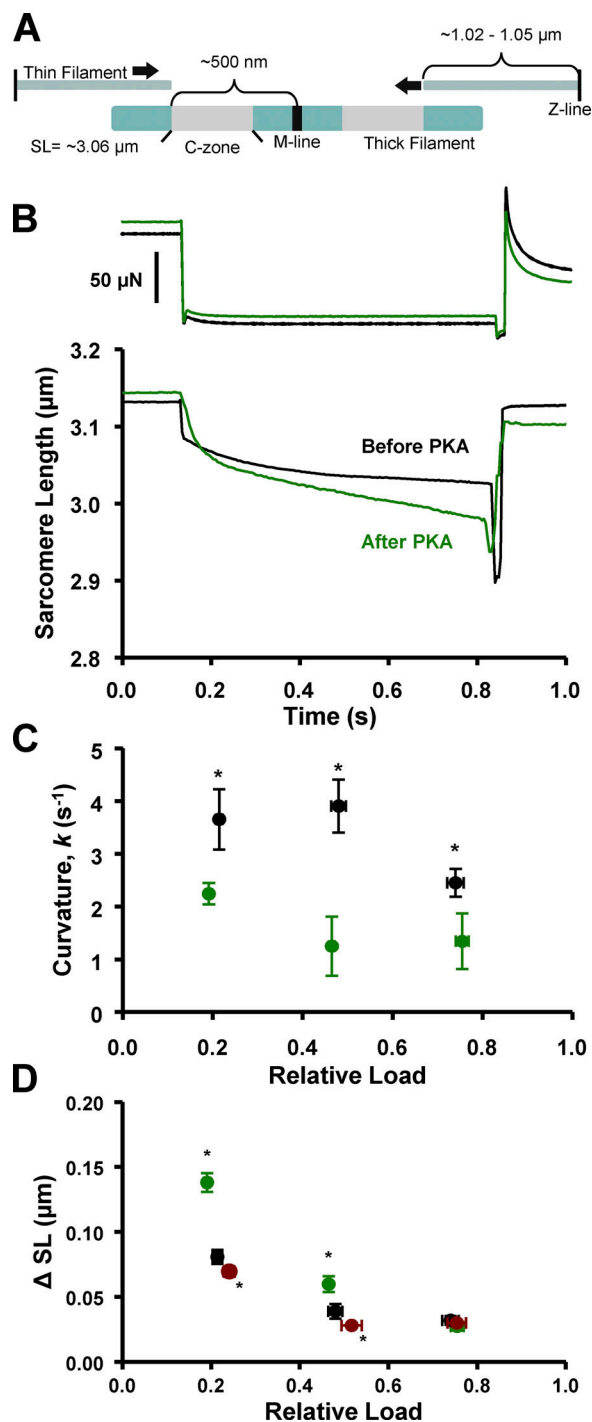


Figure 7. Effects of PKA and lambda phosphatase on SL shortening. (A) Schematic of skeletal muscle C-zone. (B) Representative force (top) and sarcomere length (bottom) during loaded shortening into the C-zone before (black) and after (green) of PKA treatment. (C and D) Summary of sarcomere length trace curvature (C) and sarcomere length shortening (D) before (black) and after (green) PKA treatment. Sarcomere length shortening was decreased following lambda phosphatase treatment (D, red). Decreased curvature and increased magnitude of sarcomere shortening implicates less deceleration and faster overall loaded shortening during force clamps ($n = 5$). *, $P < 0.05$ compared with non-PKA using paired t test analysis.

clinically significant disease states including Duchenne muscular dystrophy and arthrogryposis are associated with alterations in sMyBP-C phosphorylation (Ackermann et al., 2015a,b); (b) there are limited studies on the functional effects of skeletal isoforms of MyBP-C, especially in relation to phosphorylation levels; and (c) skeletal muscle fibers allowed for testing of molecule specificity of contractile properties, since PKA phosphorylates sMyBP-C but not slow-skeletal cTnI (Hanft et al., 2016). Regarding the latter, our laboratory has previously observed that PKA-induced phosphorylation of cMyBP-C and cTnI elicited marked increases in transient force overshoot in permeabilized cardiac myocyte preparations, which was speculated to arise from increased cooperativity of myofilament activation (Hanft and McDonald, 2009). In addition, previous work found that transient force overshoot resulted from, at least in part, cooperative recruitment of force-generating cross-bridges (Campbell, 2006b). Thus, we hypothesized that fast-twitch skeletal muscle would have a greater magnitude of transient force overshoot owing to its higher level of cooperativity compared with slow-twitch skeletal muscle (McDonald, 2000). Contrary to the hypothesis, slow-twitch skeletal muscle fibers elicited a greater magnitude of transient force overshoot than fast-twitch skeletal muscle fibers (Fig. 2 A). This suggests that while cooperative activation is involved, it is not likely the sole component that determines magnitude of transient force overshoot, and Ca^{2+} -activated slow-twitch fibers have a greater propensity for cross-bridge recruitment in response to mechanical perturbation. One potential mechanism that could explain fiber-type variation in transient force overshoot could be thin filament compliance. According to some computational models, more compliant myofilaments increase recruitment of force-generating cross-bridges (Campbell, 2006a) owing to additional realignment of myosin binding sites along the thin filament, which can lead to greater cross-bridge binding and more thin filament cooperative activation by shifting thin filaments to the open state (Daniel et al., 1998), and this process may be more predominant in slow-twitch than fast-twitch skeletal muscle fibers.

From the standpoint of regulation of striated muscle contraction, there appear to be, at least, two control systems: (1) the canonical Ca^{2+} activated thin filament pathway (Ebashi and Kodama, 1966; Greaser and Gergely, 1973; McKillop and Geeves, 1993) and (2) the more recently discovered thick filament stress-activated pathway (Linari et al., 2015; Fusi et al., 2016). MyBP-C appears to be ideally localized to serve as a mechanosensor for rapid adjustments between thin and thick filament activation in response to ligand activation, stress, and strain signals. In fact, there is considerable evidence that MyBP-C isoforms can bind both actin and myosin in a phosphorylation-dependent manner (Moss et al., 2015). cMyBP-C binding to myosin has been proposed to inhibit thick filament activation (Kampourakis et al., 2014), and its interaction with myosin is weakened by PKA phosphorylation of the serines within the M domain (Gautel et al., 1995; Ababou et al., 2008; Bhuiyan et al., 2012), which has been shown to release myosin cross-bridges from the surface of the thick filaments (Colson et al., 2008; Kensler et al., 2017). These results led us to propose a model

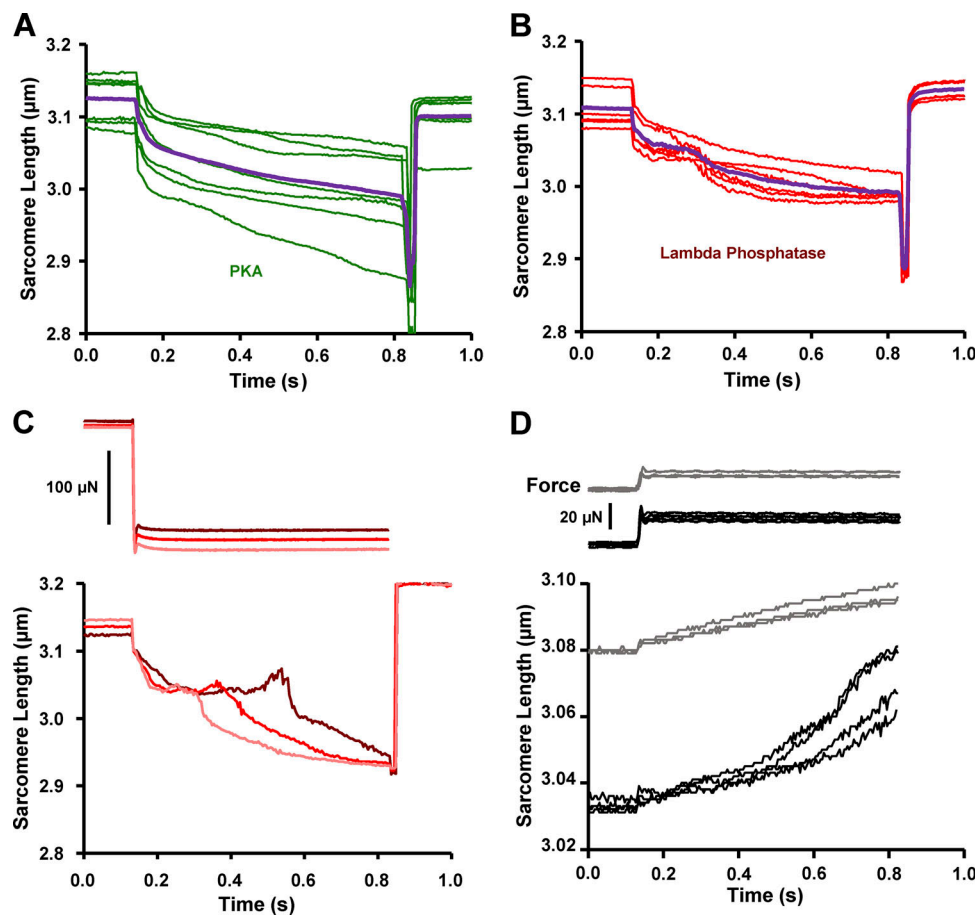


Figure 8. Sarcomere length traces exhibited a prominent “bump” during lightly loaded shortening following sMyBP-C dephosphorylation by lambda phosphatase treatment (red). (A and B) Representative sarcomere length shortening into the C-zone traces following PKA (A, green) and lambda phosphatase (B, red). Trace averages are shown in purple following PKA (A) and lambda phosphatase (B). (C) Sarcomere length trace bumps were manipulated by slight alteration of load clamps. Increasing the load clamp by ~5% intervals caused a greater time delay in the sarcomere bump, i.e., sarcomeres shortened more slowly ostensibly causing thin filaments to engage the C-zone at a later time point. (D) Sarcomere length traces exhibited a biphasic lengthening when exiting the apparent C-zone (black; $n = 3$). The rate of lengthening increased as sarcomeres lengthened beyond ~3.05 μm . When the fiber preparation was stretched to a sarcomere length of ~3.08 μm , the sarcomeres exhibited a more linear lengthening during supra-isometric load clamps (gray).

whereby sMyBP-C serves as interfilament regulator with the probability of dual interaction modulated by its phosphorylation state (Fig. 9). According to this model, unphosphorylated sMyBP-C has a higher probability of binding both actin and myosin, which would tend to attenuate both the force and rate of contraction as well as impede filament shortening. Alternatively, phosphorylation of sMyBP-C alleviates its linkage between the thin and thick filaments, which would enhance the magnitude and rate of force and speed filament sliding.

Experiments were designed to test this model in slow-twitch skeletal muscle fibers and, consistent with the model, we observed that the relative magnitude of the transient force overshoot more than doubled at low Ca^{2+} levels following PKA phosphorylation of sMyBP-C (Fig. 4 D). This result is consistent with the idea that phosphorylation of sMyBP-C relieves its constraint on myosin heads and increases the propensity for recruitment of cycling cross-bridges. It is interesting that PKA augmented the transient force overshoot only at low levels of Ca^{2+} activation. Such a result, however, seems reasonable when examined in the context of thick filament regulation of

contraction (Linari et al., 2015; Fusi et al., 2016), where it is postulated that in a relaxed state, both the thin and thick filaments are in an OFF state. Under low stress levels (e.g., low Ca^{2+} activation levels), thin filaments transition to the open or ON state while thick filaments remain in the OFF state, and as such, there is a large pool of cross-bridges capable of being recruited into the cycling, force-generating state. In contrast, at higher stress levels, thick filaments have transitioned to the ON state so the majority of cross-bridges are already in the cycling, force-generating pool. In accordance with our results, we propose that phosphorylation of sMyBP-C allows the transition of the thick filament toward the ON state, and thus, more myosin cross-bridges are available to be recruited into the cycling, force-generating pool, which manifests as a large increase in the relative magnitude of the transient force overshoot but only at low Ca^{2+} activations. However, at higher Ca^{2+} activation levels, greater stress is imposed on thick filaments, causing the transition of thick filaments to the fully ON state, and thus, phosphorylation of sMyBP-C does not elicit a further stretch-mediated increase in the relative transient force overshoot.

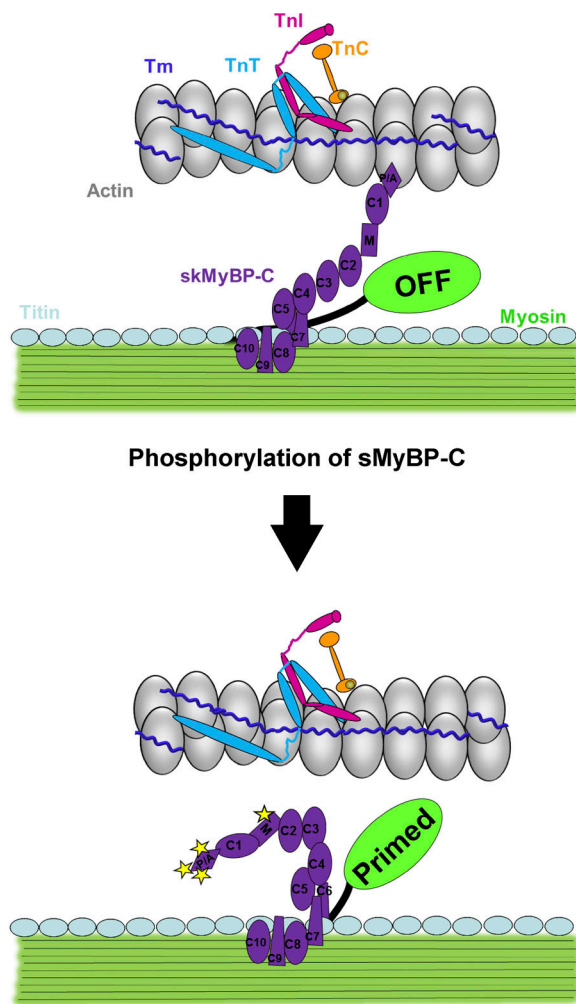


Figure 9. **Schematic of PKA-induced phosphorylation of sMyBP-C.** Unphosphorylated sMyBP-C (top) binds both actin and myosin and attenuates the rate and force of contraction as well as impedes filament shortening. The phosphorylation of sMyBP-C (bottom) alleviates its linkage between the thin and thick filament, which enhances the rate and magnitude of force and speeds filament sliding.

Alternatively, it is possible that PKA-mediated sMyBP-C phosphorylation, especially at residues in the N-terminal Pro/Ala-rich region (i.e., Ser-59), may augment transient force overshoot by activation of the thin filaments, perhaps by stereospecific binding to thin filament regions that cause azimuthal tropomyosin movement similar to those associated with Ca^{2+} activation (Whitten et al., 2008; Mun et al., 2014).

PKA-mediated phosphorylation of sMyBP-C also increased rates of force redevelopment, and this occurred at all levels of Ca^{2+} activation (Fig. 5, A and B). This result suggests that sMyBP-C regulates, in a phosphorylation state-dependent manner, the kinetics of isometric cycling myosin cross-bridges (Brenner, 1988) and/or the rate of cooperative recruitment of cycling cross-bridges (Swartz and Moss, 1992; Campbell, 1997; Campbell and Chandra, 2006; Chandra et al., 2015; Mamidi et al., 2016). It is also possible that changes in the phosphorylation state of other myofilament proteins such as regulatory myosin light chain may contribute to the decreased rates of

force development following lambda phosphatase (Fig. 6, B and C). We also found that force redevelopment traces (measured over several seconds) were better fitted with a double exponential equation, suggesting that force redevelopment involves a biphasic response (Fig. 1 E); a similar observation was previously reported for stretch activation of permeabilized myocardial preparations (Stelzer et al., 2006). Interestingly, the two phases of force redevelopment converged at low levels of Ca^{2+} activation (Fig. 3 A). It seems reasonable to suggest that the faster process (indexed by the k_1 rate constant) may reflect the cycling kinetics of cross-bridges transitioning from detached, non-force-generating to attached, force-generating states (Brenner, 1988; Wolff et al., 1995), whereas the slower process (indexed by the k_2 rate constant) may reflect cooperative recruitment of cross-bridges from the population of noncycling cross-bridges to the pool of cycling, force-generating cross-bridges (Swartz and Moss, 1992; Campbell, 1997). According to this line of reasoning, at higher levels of Ca^{2+} activation, there is a higher probability that most regions of thin and thick filaments are activated (in the open and/or ON state) such that the first-order process of cross-bridge cycling dominates force development. However, at lower levels of Ca^{2+} activation, more regions of both the thin and thick filament are in the blocked, closed, and/or OFF state and more likely to undergo the slower process of cooperative activation. This is consistent with our observation of the convergence of the two phases as Ca^{2+} activation levels were progressively lowered. Alternatively, the two phases may arise from differences between cross-bridge and half-sarcomere strain during force redevelopment, which converge at low levels of Ca^{2+} activation (Caremani et al., 2008).

As previously stated, MyBP-C is restricted to a region on the thick filament known as the C-zone. MyBP-C is located on seven to nine stripes that are spaced ~ 43 nm apart. MyBP-C itself has been shown to attenuate sarcomere shortening in permeabilized muscle preparations: for example, partial fast skeletal MyBP-C extraction increased the low-velocity phase of maximal shortening velocity in rabbit permeabilized fast-twitch skeletal muscle fibers (Hofmann et al., 1991). Also, loaded shortening and power output were markedly increased in permeabilized cardiac myocyte preparations from cMyBP-C knockout mice (Korte et al., 2003). In isolated filament assays, the addition of N-terminal fragments of MyBP-C slowed actin sliding velocity in a load-clamped laser trap assay (Weith et al., 2012), the presence of MyBP-C in native cardiac thick filaments caused a slowdown of isolated thin filaments as they traversed the C-zone, and the velocities were modulated by PKA and lambda phosphatase treatment (Previs et al., 2012). Here we extended these in vitro experiments and tested if sMyBP-C was capable of acting as a brake system as thin filaments slide into the C-zone in the context of an intact sarcomeric myofilament lattice. Before PKA treatment, the sarcomere length traces exhibited significant curvature, implying a deceleration of shortening as the thin filament slid into the C-zone (Fig. 7). PKA phosphorylation of sMyBP-C caused both a decrease in curvature and an increase in the distance shortened (Fig. 7). These results are consistent with the idea that sMyBP-C attenuates filament sliding velocity and sMyBP-C phosphorylation decreases the viscous load it imposes

on filament sliding. Next, if phosphorylation of sMyBP-C causes a decrease in the internal sarcomeric braking system, then it stands to reason that dephosphorylation of sMyBP-C would increase drag. Thus, we treated the slow-twitch skeletal muscle fibers with lambda phosphatase to dephosphorylate sMyBP-C. Interestingly, after sMyBP-C dephosphorylation, sarcomere shortening started to decelerate and often elicited a bump in shortening as the thin filament slid into the C-zone (at SL = ~3.08–3.04 μm ; Fig. 8 B). It seems reasonable that the bump occurs when the thin filaments first interact with sMyBP-C in the C-zone. Consistent with this, for a given preparation, the bump occurred at the same SL independent of time during force clamps (Fig. 8 C). Remarkably, dephosphorylated MyBP-C's putative interaction with actin appeared to be forceful enough to actually stop sarcomere shortening momentarily and cause filaments to recoil, as evident by SL extension (Fig. 8). These SL traces were somewhat peculiar, because the motor length shortening trace did not exhibit bumps. One potential explanation for these discordant results is the presence of sarcomere shortening heterogeneity along the fiber. Two potential consequences of sarcomere shortening heterogeneity are (a) if the sarcomeres in the middle of the fiber are undergoing a recoil (i.e., extension), then sarcomeres at the ends of the fiber should display a simultaneous amplification of shortening; and (b) individual half-sarcomeres will enter the C-zone at slightly different times. Both of these phenomena could account for the discordant observations between average SL recordings and motor position recordings. The discernment of either of these possibilities was not determined in the present study and would necessitate resolution at the half-sarcomere level to firmly establish whether half-sarcomere shortening can actually stop and recoil when sliding thin filaments abut against dephosphorylated MyBP-C molecules that span the interfilament space. Computational modeling of half-sarcomere behavior in the presence of internal loads also is needed to address the likelihood that thin filament–sMyBP-C interactions can yield such abrupt strains during loaded shortening of Ca^{2+} activated myofilaments, as implicated from the findings. One limitation of these interpretations is that thin filament lengths of rat soleus slow-twitch skeletal muscle fibers, to our knowledge, have not been measured and were assumed to be ~1.02–1.05 μm from a study in rat skeletal muscle (Greaser and Pleitner, 2014). However, the aforementioned study did not provide thin filament lengths from the rat soleus muscle per se, and a previous report observed thin filaments in slow-twitch muscle to be slightly longer than in fast twitch muscle, at least in mouse (Li et al., 2015). Future studies are needed to measure thin filament lengths in rat soleus slow-twitch muscle fibers.

Overall, these results suggest that sMyBP-C acts as a variable gain attenuator of force and power and that its phosphorylation by PKA leads to elevated force, loaded shortening, and power by a combination of recruitment of cross-bridges, faster cross-bridge cycling kinetics, and reduction in drag forces as thin filaments slide through the C-zone. The biophysical findings from this study may (a) provide mechanistic insight into the precision and efficiency by which striated muscle dynamically functions and (b) help explain some of the pathophysiology

associated with diseases such as arthrogryposis myopathy, whereby mutations in sMyBP-C cause haploinsufficiency and/or altered phosphorylation states that correspond with severe muscle deformations and tremors (Ackermann et al., 2015b; Geist and Kontrogianni-Konstantopoulos, 2016).

Acknowledgments

This work was supported by a National Heart, Lung, and Blood Institute grant (R01-HL-57852) and University of Missouri School of Medicine Bridge Funding to K.S. McDonald. The work was also supported by the National Institutes of Health/National Institute of Arthritis and Musculoskeletal and Skin Diseases (Training Program in Muscle Biology, T32 AR007592-17 to J. Geist and R21AR072981 to A. Kontrogianni-Konstantopoulos) and the Muscular Dystrophy Association (research grant 313579 to A. Kontrogianni-Konstantopoulos). The content is solely the responsibility of the authors and does not necessarily represent the official views of the National Institutes of Health and the Muscular Dystrophy Association.

The authors declare no competing financial interests.

Author contributions: All experiments were performed in the laboratory of K.S. McDonald. J.C. Robinett and K.S. McDonald contributed equally in concept and design of experiments, collection, analysis, and interpretation of data, and drafting and revising of manuscript. L.M. Hanft performed western blot analysis and assisted in concept and design of experiments, data analysis, and drafting and revising the manuscript. J. Geist and A. Kontrogianni-Konstantopoulos provided antibodies for assessment of sMyBP-C residue specific phosphorylation analysis and assisted in revising the manuscript.

Henk L. Granzier served as editor.

Submitted: 1 August 2018

Accepted: 11 January 2019

References

- Ababou, A., E. Rostkova, S. Mistry, C. Le Masurier, M. Gautel, and M. Pfuhl. 2008. Myosin binding protein C positioned to play a key role in regulation of muscle contraction: structure and interactions of domain C1. *J. Mol. Biol.* 384:615–630. <https://doi.org/10.1016/j.jmb.2008.09.065>
- Ackermann, M.A., and A. Kontrogianni-Konstantopoulos. 2011. Myosin binding protein-C slow is a novel substrate for protein kinase A (PKA) and C (PKC) in skeletal muscle. *J. Proteome Res.* 10:4547–4555. <https://doi.org/10.1021/pr200355w>
- Ackermann, M.A., and A. Kontrogianni-Konstantopoulos. 2013. Myosin binding protein-C slow: a multifaceted family of proteins with a complex expression profile in fast and slow twitch skeletal muscles. *Front. Physiol.* 4:391. <https://doi.org/10.3389/fphys.2013.00391>
- Ackermann, M.A., J.P. Kerr, B. King, C. W Ward, and A. Kontrogianni-Konstantopoulos. 2015a. The Phosphorylation Profile of Myosin Binding Protein-C Slow is Dynamically Regulated in Slow-Twitch Muscles in Health and Disease. *Sci. Rep.* 5:12637. <https://doi.org/10.1038/srep12637>
- Ackermann, M.A., C.W. Ward, C. Gurnett, and A. Kontrogianni-Konstantopoulos. 2015b. Myosin Binding Protein-C Slow Phosphorylation is Altered in Duchenne Dystrophy and Arthrogryposis Myopathy in Fast-Twitch Skeletal Muscles. *Sci. Rep.* 5:13235. <https://doi.org/10.1038/srep13235>
- Barefield, D., and S. Sadayappan. 2010. Phosphorylation and function of cardiac myosin binding protein-C in health and disease. *J. Mol. Cell. Cardiol.* 48:866–875. <https://doi.org/10.1016/j.yjmcc.2009.11.014>

- Bennett, P., R. Craig, R. Starr, and G. Offer. 1986. The ultrastructural location of C-protein, X-protein and H-protein in rabbit muscle. *J. Muscle Res. Cell Motil.* 7:550–567. <https://doi.org/10.1007/BF01753571>
- Bhuiyan, M.S., J. Gulick, H. Osinska, M. Gupta, and J. Robbins. 2012. Determination of the critical residues responsible for cardiac myosin binding protein C's interactions. *J. Mol. Cell. Cardiol.* 53:838–847. <https://doi.org/10.1016/j.yjmcc.2012.08.028>
- Brenner, B. 1988. Effect of Ca²⁺ on cross-bridge turnover kinetics in skinned single rabbit psoas fibers: implications for regulation of muscle contraction. *Proc. Natl. Acad. Sci. USA.* 85:3265–3269. <https://doi.org/10.1073/pnas.85.9.3265>
- Campbell, K. 1997. Rate constant of muscle force redevelopment reflects cooperative activation as well as cross-bridge kinetics. *Biophys. J.* 72:254–262. [https://doi.org/10.1016/S0006-3495\(97\)78664-8](https://doi.org/10.1016/S0006-3495(97)78664-8)
- Campbell, K.S. 2006a. Filament compliance effects can explain tension overshoots during force development. *Biophys. J.* 91:4102–4109. <https://doi.org/10.1529/biophysj.106.087312>
- Campbell, K.S. 2006b. Tension recovery in permeabilized rat soleus muscle fibers after rapid shortening and restretch. *Biophys. J.* 90:1288–1294. <https://doi.org/10.1529/biophysj.105.067504>
- Campbell, K.B., and M. Chandra. 2006. Functions of stretch activation in heart muscle. *J. Gen. Physiol.* 127:89–94. <https://doi.org/10.1085/jgp.200509483>
- Caremani, M., J. Dantzig, Y.E. Goldman, V. Lombardi, and M. Linari. 2008. Effect of inorganic phosphate on the force and number of myosin cross-bridges during the isometric contraction of permeabilized muscle fibers from rabbit psoas. *Biophys. J.* 95:5798–5808. <https://doi.org/10.1529/biophysj.108.130435>
- Chandra, V., S.K. Gollapudi, and M. Chandra. 2015. Rat cardiac troponin T mutation (F72L)-mediated impact on thin filament cooperativity is divergently modulated by α - and β -myosin heavy chain isoforms. *Am. J. Physiol. Heart Circ. Physiol.* 309:H1260–H1270. <https://doi.org/10.1152/ajpheart.00519.2015>
- Colson, B.A., T. Bekyarova, M.R. Locher, D.P. Fitzsimons, T.C. Irving, and R.L. Moss. 2008. Protein kinase A-mediated phosphorylation of cMyBP-C increases proximity of myosin heads to actin in resting myocardium. *Circ. Res.* 103:244–251. <https://doi.org/10.1161/CIRCRESAHA.108.178996>
- Colson, B.A., J.R. Patel, P.P. Chen, T. Bekyarova, M.I. Abdalla, C.W. Tong, D.P. Fitzsimons, T.C. Irving, and R.L. Moss. 2012. Myosin binding protein-C phosphorylation is the principal mediator of protein kinase A effects on thick filament structure in myocardium. *J. Mol. Cell. Cardiol.* 53:609–616. <https://doi.org/10.1016/j.yjmcc.2012.07.012>
- Craig, R., and G. Offer. 1976. The location of C-protein in rabbit skeletal muscle. *Proc. R. Soc. Lond. B Biol. Sci.* 192:451–461. <https://doi.org/10.1098/rspb.1976.0023>
- Daniel, T.L., A.C. Trimble, and P.B. Chase. 1998. Compliant realignment of binding sites in muscle: transient behavior and mechanical tuning. *Biophys. J.* 74:1611–1621. [https://doi.org/10.1016/S0006-3495\(98\)77875-0](https://doi.org/10.1016/S0006-3495(98)77875-0)
- Ebashi, S., and A. Kodama. 1966. Native tropomyosin-like action of troponin on trypsin-treated myosin B. *J. Biochem.* 60:733–734. <https://doi.org/10.1093/oxfordjournals.jbchem.a128504>
- Flashman, E., C. Redwood, J. Moolman-Smook, and H. Watkins. 2004. Cardiac myosin binding protein C: its role in physiology and disease. *Circ. Res.* 94:1279–1289. <https://doi.org/10.1161/01.RES.0000127175.21818.C2>
- Fusi, L., E. Brunello, Z. Yan, and M. Irving. 2016. Thick filament mechanosensing is a calcium-independent regulatory mechanism in skeletal muscle. *Nat. Commun.* 7:13281. <https://doi.org/10.1038/ncomms13281>
- Gautel, M., O. Zuffardi, A. Freiburg, and S. Labeit. 1995. Phosphorylation switches specific for the cardiac isoform of myosin binding protein-C: a modulator of cardiac contraction? *EMBO J.* 14:1952–1960. <https://doi.org/10.1002/j.1460-2075.1995.tb07187.x>
- Geist, J., and A. Kontrogianni-Konstantopoulos. 2016. MYBPC1, an Emerging Myopathic Gene: What We Know and What We Need to Learn. *Front. Physiol.* 7:410. <https://doi.org/10.3389/fphys.2016.00410>
- Greaser, M.L., and J. Gergely. 1973. Purification and properties of the components from troponin. *J. Biol. Chem.* 248:2125–2133.
- Greaser, M.L., and J.M. Pleitner. 2014. Titin isoform size is not correlated with thin filament length in rat skeletal muscle. *Front. Physiol.* 5:35. <https://doi.org/10.3389/fphys.2014.00035>
- Gresham, K.S., R. Mamidi, and J.E. Stelzer. 2014. The contribution of cardiac myosin binding protein-c Ser282 phosphorylation to the rate of force generation and in vivo cardiac contractility. *J. Physiol.* 592:3747–3765. <https://doi.org/10.1113/jphysiol.2014.276022>
- Hanft, L.M., and K.S. McDonald. 2009. Sarcomere length dependence of power output is increased after PKA treatment in rat cardiac myocytes. *Am. J. Physiol. Heart Circ. Physiol.* 296:H1524–H1531. <https://doi.org/10.1152/ajpheart.00864.2008>
- Hanft, L.M., T.D. Cornell, C.A. McDonald, M.J. Rovetto, C.A. Emter, and K.S. McDonald. 2016. Molecule specific effects of PKA-mediated phosphorylation on rat isolated heart and cardiac myofibrillar function. *Arch. Biochem. Biophys.* 601:22–31. <https://doi.org/10.1016/j.abb.2016.01.019>
- Harris, S.P., R.G. Lyons, and K.L. Bezold. 2011. In the thick of it: HCM-causing mutations in myosin binding proteins of the thick filament. *Circ. Res.* 108:751–764. <https://doi.org/10.1161/CIRCRESAHA.110.231670>
- Hartzell, H.C., and W.S. Sale. 1985. Structure of C protein purified from cardiac muscle. *J. Cell Biol.* 100:208–215. <https://doi.org/10.1083/jcb.100.1.208>
- Hofmann, P.A., M.L. Greaser, and R.L. Moss. 1991. C-protein limits shortening velocity of rabbit skeletal muscle fibres at low levels of Ca²⁺ activation. *J. Physiol.* 439:701–715. <https://doi.org/10.1113/jphysiol.1991.sp018689>
- Kampourakis, T., Z. Yan, M. Gautel, Y.-B. Sun, and M. Irving. 2014. Myosin binding protein-C activates thin filaments and inhibits thick filaments in heart muscle cells. *Proc. Natl. Acad. Sci. USA.* 111:18763–18768. <https://doi.org/10.1073/pnas.1413922112>
- Kensler, R.W., J.F. Shaffer, and S.P. Harris. 2011. Binding of the N-terminal fragment C0-C2 of cardiac MyBP-C to cardiac F-actin. *J. Struct. Biol.* 174:44–51. <https://doi.org/10.1016/j.jsb.2010.12.003>
- Kensler, R.W., R. Craig, and R.L. Moss. 2017. Phosphorylation of cardiac myosin binding protein C releases myosin heads from the surface of cardiac thick filaments. *Proc. Natl. Acad. Sci. USA.* 114:E1355–E1364. <https://doi.org/10.1073/pnas.1614020114>
- Korte, F.S., K.S. McDonald, S.P. Harris, and R.L. Moss. 2003. Loaded shortening, power output, and rate of force redevelopment are increased with knockout of cardiac myosin binding protein-C. *Circ. Res.* 93:752–758. <https://doi.org/10.1161/01.RES.0000096363.85588.9A>
- Lee, K., S.P. Harris, S. Sadayappan, and R. Craig. 2015. Orientation of myosin binding protein C in the cardiac muscle sarcomere determined by domain-specific immuno-EM. *J. Mol. Biol.* 427:274–286. <https://doi.org/10.1016/j.jmb.2014.10.023>
- Li, F., D. Buck, J. De Winter, J. Kolb, H. Meng, C. Birch, R. Slater, Y.N. Escobar, J.E. Smith III, L. Yang, et al. 2015. Nebulin deficiency in adult muscle causes sarcomere defects and muscle-type-dependent changes in trophicity: novel insights in nemaline myopathy. *Hum. Mol. Genet.* 24:5219–5233. <https://doi.org/10.1093/hmg/ddv243>
- Linari, M., E. Brunello, M. Reconditi, L. Fusi, M. Caremani, T. Narayanan, G. Piazzesi, V. Lombardi, and M. Irving. 2015. Force generation by skeletal muscle is controlled by mechanosensing in myosin filaments. *Nature.* 528:276–279. <https://doi.org/10.1038/nature15727>
- Luther, P.K., H. Winkler, K. Taylor, M.E. Zoghbi, R. Craig, R. Padrón, J.M. Squire, and J. Liu. 2011. Direct visualization of myosin-binding protein C bridging myosin and actin filaments in intact muscle. *Proc. Natl. Acad. Sci. USA.* 108:11423–11428. <https://doi.org/10.1073/pnas.1103216108>
- Mamidi, R., E.S. Gresham, S. Verma, and J.E. Stelzer. 2016. Cardiac myosin binding protein-C phosphorylation modulates myofilament length-dependent activation. *Front. Physiol.* 7:38. <https://doi.org/10.3389/fphys.2016.00038>
- McDonald, K.S. 2000. Ca²⁺ dependence of loaded shortening in rat skinned cardiac myocytes and skeletal muscle fibres. *J. Physiol.* 525:169–181. <https://doi.org/10.1111/j.1469-7793.2000.00169.x>
- McKillop, D.F., and M.A. Geeves. 1993. Regulation of the interaction between actin and myosin subfragment 1: evidence for three states of the thin filament. *Biophys. J.* 65:693–701. [https://doi.org/10.1016/S0006-3495\(93\)81110-X](https://doi.org/10.1016/S0006-3495(93)81110-X)
- Moos, C., C.M. Mason, J.M. Besterman, I.N. Feng, and J.H. Dubin. 1978. The binding of skeletal muscle C-protein to F-actin, and its relation to the interaction of actin with myosin subfragment-1. *J. Mol. Biol.* 124:571–586. [https://doi.org/10.1016/0022-2836\(78\)90172-9](https://doi.org/10.1016/0022-2836(78)90172-9)
- Moss, R.L., D.P. Fitzsimons, and J.C. Ralphe. 2015. Cardiac MyBP-C regulates the rate and force of contraction in mammalian myocardium. *Circ. Res.* 116:183–192. <https://doi.org/10.1161/CIRCRESAHA.116.300561>
- Mun, J.Y., M.J. Previs, H.Y. Yu, J. Gulick, L.S. Tobacman, S. Beck Previs, J. Robbins, D.M. Warshaw, and R. Craig. 2014. Myosin-binding protein C displaces tropomyosin to activate cardiac thin filaments and governs their speed by an independent mechanism. *Proc. Natl. Acad. Sci. USA.* 111:2170–2175. <https://doi.org/10.1073/pnas.1316001111>
- Patel, J.R., D.P. Fitzsimons, S.H. Buck, M. Muthuchamy, D.F. Wiczorek, and R.L. Moss. 2001. PKA accelerates rate of force development in murine skinned myocardium expressing alpha- or beta-tropomyosin. *Am. J. Physiol. Heart Circ. Physiol.* 280:H2732–H2739. <https://doi.org/10.1152/ajpheart.2001.280.6.H2732>

- Pepe, F.A., and B. Drucker. 1975. The myosin filament. III. C-protein. *J. Mol. Biol.* 99:609–617. [https://doi.org/10.1016/S0022-2836\(75\)80175-6](https://doi.org/10.1016/S0022-2836(75)80175-6)
- Piazzesi, G., M. Reconditi, M. Linari, L. Lucii, P. Bianco, E. Brunello, V. De-costre, A. Stewart, D.B. Gore, T.C. Irving, et al. 2007. Skeletal muscle performance determined by modulation of number of myosin motors rather than motor force or stroke size. *Cell.* 131:784–795. <https://doi.org/10.1016/j.cell.2007.09.045>
- Previs, M.J., S. Beck Previs, J. Gulick, J. Robbins, and D.M. Warshaw. 2012. Molecular mechanics of cardiac myosin-binding protein C in native thick filaments. *Science.* 337:1215–1218. <https://doi.org/10.1126/science.1223602>
- Reconditi, M., E. Brunello, L. Fusi, M. Linari, M.F. Martinez, V. Lombardi, M. Irving, and G. Piazzesi. 2014. Sarcomere-length dependence of myosin filament structure in skeletal muscle fibres of the frog. *J. Physiol.* 592: 1119–1137. <https://doi.org/10.1113/jphysiol.2013.267849>
- Rybakova, I.N., M.L. Greaser, and R.L. Moss. 2011. Myosin binding protein C interaction with actin: characterization and mapping of the binding site. *J. Biol. Chem.* 286:2008–2016. <https://doi.org/10.1074/jbc.M110.170605>
- Shaffer, J.F., R.W. Kensler, and S.P. Harris. 2009. The myosin-binding protein C motif binds to F-actin in a phosphorylation-sensitive manner. *J. Biol. Chem.* 284:12318–12327. <https://doi.org/10.1074/jbc.M808850200>
- Sarr, R., and G. Offer. 1978. The interaction of C-protein with heavy mero-myosin and subfragment-2. *Biochem. J.* 171:813–816. <https://doi.org/10.1042/bj1710813>
- Stelzer, J.E., and R.L. Moss. 2006. Contributions of stretch activation to length-dependent contraction in murine myocardium. *J. Gen. Physiol.* 128:461–471.
- Stelzer, J.E., L. Larsson, D.P. Fitzsimons, and R.L. Moss. 2006. Activation dependence of stretch activation in mouse skinned myocardium: implications for ventricular function. *J. Gen. Physiol.* 127:95–107.
- Swartz, D.R., and R.L. Moss. 1992. Influence of a strong-binding myosin analogue on calcium-sensitive mechanical properties of skinned skeletal muscle fibers. *J. Biol. Chem.* 267:20497–20506.
- van Dijk, S.J., K.L. Bezold, and S.P. Harris. 2014. Earning stripes: myosin binding protein-C interactions with actin. *Pflugers Arch.* 466:445–450. <https://doi.org/10.1007/s00424-013-1432-8>
- Walcott, S., S. Docken, and S.P. Harris. 2015. Effects of cardiac Myosin binding protein-C on actin motility are explained with a drag-activation-competition model. *Biophys. J.* 108:10–13. <https://doi.org/10.1016/j.bpj.2014.11.1852>
- Wang, L., J. Geist, A. Grogan, L.R. Hu, and A. Kontogianni-Konstantopoulos. 2018. Thick Filament Protein Network, Functions, and Disease Association. *Compr. Physiol.* 8:631–709. <https://doi.org/10.1002/cphy.c170023>
- Weith, A.E., M.J. Previs, G.J. Hoepflich, S.B. Previs, J. Gulick, J. Robbins, and D. M. Warshaw. 2012. The extent of cardiac myosin binding protein-C phosphorylation modulates actomyosin function in a graded manner. *J. Muscle Res. Cell Motil.* 33:449–459. <https://doi.org/10.1007/s10974-012-9312-y>
- Whitten, A.E., C.M. Jeffries, S.P. Harris, and J. Trewthella. 2008. Cardiac myosin-binding protein C decorates F-actin: implications for cardiac function. *Proc. Natl. Acad. Sci. USA.* 105:18360–18365. <https://doi.org/10.1073/pnas.0808903105>
- Wolff, M.R., K.S. McDonald, and R.L. Moss. 1995. Rate of tension development in cardiac muscle varies with level of activator calcium. *Circ. Res.* 76: 154–160. <https://doi.org/10.1161/01.RES.76.1.154>
- Yamamoto, K. 1986. The binding of skeletal muscle C-protein to regulated actin. *FEBS Lett.* 208:123–127. [https://doi.org/10.1016/0014-5793\(86\)81545-9](https://doi.org/10.1016/0014-5793(86)81545-9)
- Yamamoto, K., and C. Moos. 1983. The C-proteins of rabbit red, white, and cardiac muscles. *J. Biol. Chem.* 258:8395–8401.